

# Investigation of ionization of positive ions by electron impact

E. D. Donets and V. P. Ovsyannikov

Joint Institute for Nuclear Research

(Submitted 17 June 1980)

Zh. Éksp. Teor. Fiz. **80**, 916–925 (March 1981)

A method is described for measurement of the effective cross sections for ionization of positive ions by electron impact in an electrostatic ion trap produced by the space charge of an electron beam. The results of measurement of the energy dependences of the cross sections for all C, N, O, and Ne positive ions (excluding  $\text{Ne}^+$ ) are presented for electron energies from 2 to 8–10 keV. Values of the effective cross sections are obtained for Ar ions (from  $\text{Ar}^{3+}$  to  $\text{Ar}^{17+}$ ) at electron energies 11 keV; the cross sections for the  $\text{Ar}^{15+}$ ,  $\text{Ar}^{16+}$ , and  $\text{Ar}^{17+}$  ions are also measured for 7.8 keV electrons. Qualitative results are obtained by measuring the ionization cross sections for Kr (up to  $\text{Kr}^{33+}$ ) and for Xe (up to  $\text{Xe}^{47+}$ ). The experimental and theoretical cross sections are compared.

PACS numbers: 79.20.Kz, 79.70.+q, 72.20.Jv

## INTRODUCTION

Recently there has been considerable interest in the investigation of ionization of positive ions by electron impact. Knowledge of the effective cross sections  $\sigma_{q \rightarrow q+1}$  for ionization of ions with charge  $q$  on collision with fast electrons over a wide range of  $q$  for many elements and electron energies ( $E_e$ ) is necessary at present for diagnostics of high-temperature plasma of both terrestrial and cosmic origin, for successful development of multiply-charged ion sources, etc. A review of the theoretical aspects of the problem is given, for example, in the recent works of Bazylev and Chibisov.<sup>1,2</sup>

Up until recently, the basic method for experimental measurement of the effective cross sections  $\sigma_{q \rightarrow q+1}$  was the method of intersecting ion and electron beams (Ref. 3, p. 337). The basic advantage of this method is the better energy resolution<sup>4</sup> and the basic disadvantage is the relatively low sensitivity. As a result, up until recently the processes studied experimentally were those with participation of ions that were not more than doubly or triply charged.<sup>5–7</sup> Only in 1979 did the work of Crandall *et al.*<sup>8</sup> appear, where a Penning type source was used as the ion source, and investigations were initiated of somewhat more highly charged ions. Our work is a continuation of experiments begun earlier<sup>9–12</sup> both in terms of improving the technique and extending the scope of the investigations.

Below we present a description of the measurement technique and the results for all the positive ions of C, N, O, Ne, and Ar except for  $\text{Ne}^{1+}$  and  $\text{Ar}^{1+}$ ,<sup>2+</sup>, and also qualitative results for Kr and Xe. The experimental values are compared with those theoretical values that are available.

## 1. GENERAL DESCRIPTION OF THE TECHNIQUE

The technique development and the experiments for measurement of effective ionization cross sections were carried out on a cryogenic electron-beam ionizer which was specially designed for our purposes, the "Krion-2" (Ref. 9), the construction of which duplicates in general outline the construction of the "Krion" ionizer.<sup>10,11</sup> The

measurement technique has also been described previously.<sup>11,12</sup> Therefore, in the presentation of the technical material below, the focus is on the development of the technique, with the goal of obtaining reliable results.

A batch of the ions of the element under study was introduced at the initial instant into the electron beam within a time usually between 0.1–1 ms. As a rule, toward the end of the injection the electron beam contained a mixture of ions with relatively low charge ( $1 \leq q \leq 4$ ). The ions were held in an electrostatic trap and subjected to bombardment by beam electrons having a definite energy ( $E_e$ ). This increased the charge of the ions, and if the electron energy was sufficiently high, all the ions could be completely stripped of orbital electrons.

The charge composition of the ions directly after termination of injection was measured by a time-of-flight spectrometer (TOFS). In order to do this, all the ions were removed from the ionization region and guided to the TOFS. The current signal from the ion bunch at the outlet of the ionizer had a half-width of 40–50  $\mu\text{s}$ . A narrow temporal packet of ions  $\sim 100$  ns was skimmed for time-of-flight analysis. Therefore, to obtain reliable information concerning the ion charge distribution over the entire ion bunch, 5–6 cycles were necessary; different temporal portions of the ion signal were sampled each time. The TOFS usually operated in the current regime, so that the amplitude of each line in the charge spectrum registered on the oscilloscope screen was proportional to the total electrical charge of the ions of a given charge in the packet.

The charge spectrum was transformed into the distribution (normalized to unity) of the number of ions in the bunch by charges (the charge distribution) as follows:

$$n_q = \frac{1}{q} \sum_{k=1}^a A_q^k / \sum_{q_{\min}}^{q_{\max}} \frac{1}{q} \sum_{k=1}^a A_q^k, \quad \sum_{q_{\min}}^{q_{\max}} n_q = 1,$$

where  $n_q$  is the number of ions of charge  $q$ , normalized to unity;  $A_q^k$  is the amplitude of the line of the packet of ions of charge  $q$  in the  $k$ th sampling;  $a$  is the

number of samplings;  $q_{\min}$  and  $q_{\max}$  are the minimum and maximum charges of the ions in the bunch. The charge distribution obtained in this way was used as the initial distribution. At any moment in time, reckoned from the end of the injection process ( $\tau_i$ ) of another ionization cycle similar to the initial one, the new charge distribution of the ions in the electron beam trap can be measured. The form of this distribution, all other parameters being fixed, is determined only by the quantity  $\tau_i$  (which is given) and by the effective ionization cross sections, which alone remain unknown and are extracted from the measurement results.

In the description of the kinetics of the ionization process, in all cases except for ionization of metastable ions, the ion-electron interaction times  $\tau_i$  and the electron current density in the beam  $j$  play a common role. Therefore it is convenient to use the ionization factor  $j\tau_i$  as the variable.

If we assume that in a single collision of an electron with an ion removal of from one to several electrons is possible, then the kinetic equation for the number of ions  $n_q$  has the following form:

$$\frac{dn_q}{d(j\tau_i)} = - \sum_{f=1}^{f_{\max}} n_q \sigma_{q \rightarrow q+f} + \sum_{r=1}^{r_{\max}} n_{q-r} \sigma_{q-r \rightarrow q}, \quad (1)$$

where  $f$  and  $f_{\max}$  are the number and the maximum possible number of electrons simultaneously removed from the ion of charge  $q$ , and  $\sigma_{q \rightarrow q+f}$  is the cross section of such a process;  $r$  and  $r_{\max}$  are the number and the maximum possible number of electrons simultaneously removed from an ion of charge  $q-r$ , while  $\sigma_{q-r \rightarrow q}$  is the cross section of such a process. In the special case of successive ionization

$$dn_q/d(j\tau_i) = -n_q \sigma_{q \rightarrow q+1} + n_{q-1} \sigma_{q-1 \rightarrow q}. \quad (1a)$$

In order to determine all the unknown quantities  $\sigma$  entering in Eq. (1), it is convenient to experimentally measure the functional dependence  $n_q = f(j\tau_i)$  for all the  $q$ 's in the equation—i.e., to obtain the pattern of the charge-distribution evolution. As an example, on Fig. 1 we present the experimentally obtained charge-distribution evolution of nitrogen ions. We can draw through the evolution pattern just as many vertical sections as are necessary to obtain from the experimental data all the coefficients  $[n_q, dn_q/d(j\tau_i)]$  of the system of  $x$  equations (1), if we are looking for  $x$  unknowns  $\sigma$ . In this case, system (1) is canonical and the uniqueness of the solution of the inverse ionization problem is not

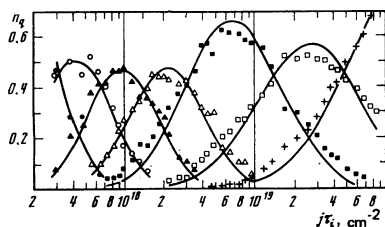


FIG. 1. Charge distribution evolution pattern for the nitrogen ions ( $E_e = 5.45$  keV):  $\bullet$ —1+,  $\circ$ —2+,  $\blacktriangle$ —3+,  $\triangle$ —4+,  $\blacksquare$ —5+,  $\square$ —6+,  $\times$ —7+.

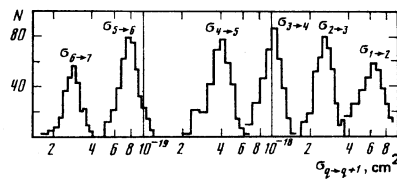


FIG. 2. Histograms of the values of  $\sigma_{q \rightarrow q+1}$  for the nitrogen ions ( $E_e = 5.45$  keV):  $\sigma_{8 \rightarrow 7} = 2.9 \pm 0.4$ ;  $\sigma_{5 \rightarrow 6} = 8.0 \pm 1.3$ ;  $\sigma_{4 \rightarrow 5} = 40 \pm 8$ ;  $\sigma_{3 \rightarrow 4} = 103 \pm 19$ ;  $\sigma_{2 \rightarrow 3} = 260 \pm 40$ ;  $\sigma_{1 \rightarrow 2} = 600 \pm 120$ .

in doubt, but finding the value of the error  $\Delta\sigma$  is quite complicated. If we recognize that the evolution pattern is usually much richer in information than is necessary for the case indicated above, i.e., we may draw more different vertical sections, then it is possible to construct several ( $M$ ) systems of equations (1), and the solution of each system yield gives its own set of  $x$  unknowns  $\sigma$ . If we consider all  $M$  systems as on an equal footing for determining the unknown  $\sigma$ , then as a result we obtain  $M$  values for each  $\sigma$ . These  $M$  values determine some value of  $\sigma$  averaged over the entire experiment (for all  $j\tau_i$ ) and the probable deviation  $\Delta\sigma$  from this value.

For illustration, the charge distribution evolution for nitrogen (Fig. 1) is worked out in a successive ionization model, in accord with the system of equations (1a). On Fig. 2, we present the histograms of the quantities  $\sigma_{q \rightarrow q+1}$  (the number of values per interval) and indicate the values of  $\sigma_{q \rightarrow q+1} \pm \Delta\sigma_{q \rightarrow q+1}$  thus obtained.

Bochev and coauthors<sup>13,14</sup> considered mathematical models of multiple ionization of positive ions by electron impact in an ion trap. The solution of the inverse problem yields a set of  $\sigma$  such that when substituted in the direct problem yields the smallest deviation of the charge distribution evolution pattern regenerated in this way from the experimental pattern. Bochev and coauthors found an approximate solution of the inverse problem on the basis of regularized iteration processes of the Gauss-Newton type.<sup>15</sup> In order to obtain numerical results on the computer, Bochev *et al.*<sup>14</sup> designed the program CHARGE based on the program COMPIL.<sup>16,17</sup> A complication arises in this case when it comes to proving the uniqueness of the solution to which the regularized iteration process converges. As a result of the reduction of the experimental data obtained for the charge-distribution evolution patterns of the nitrogen ions (see Fig. 1) by the CHARGE program, the following values of the cross sections for successive ionization were obtained:  $\sigma_{1 \rightarrow 2} = 670 \pm 90$ ,

$\sigma_{2 \rightarrow 3} = 255 \pm 45$ ,  $\sigma_{3 \rightarrow 4} = 100 \pm 11$ ,  $\sigma_{4 \rightarrow 5} = 43 \pm 3$ ,  $\sigma_{5 \rightarrow 6} = 7.5 \pm 0.5$ ,  $\sigma_{6 \rightarrow 7} = 2.8 \pm 0.4$  (in units of  $10^{-20}$  cm<sup>2</sup>). Comparing these values with those presented on Fig. 2, we see that both methods of data reduction give results which agree within the error limits.

The choice of an ionization model in which the inverse problem is solved may be substantiated in each concrete case. But, of course, the solution of the most general system of equations (1) with all the energy-allowed  $f_{\max}$  and  $r_{\max}$  would be ideal. Then the lack in

one case or another of an appreciable contributions of two-, three-, (and more) electron ionization to the charge distribution evolution would correspond to proximity of the corresponding effective cross section to zero.

In the experimental investigations it was observed that in the general case the ionization process is characterized by a certain ion-loss rate from the trap. And the higher the loss rate, the more slowly do the charge distributions evolve. Accounting for these phenomena is of primary importance for analysis of the charge distribution evolution with the goal of extracting the effective ionization cross sections. It was established experimentally that the loss rate increases sharply as the value of the electron-beam current  $I_e$  approaches some critical value  $I_e^c$ , and the loss rate is greater at a greater level of electron space charge compensation by the ion space charge  $\eta$ . Accordingly, the charge distribution evolution patterns were always obtained at  $I_e < I_e^c$ , and the dependence of the charge distribution evolution pattern on the degree of compensation was specially studied. In particular, we obtained the charge distribution evolution patterns for nitrogen ions at  $E_e = 5.45$  keV over a wide range of the initial degree of compensation  $\eta_{\tau_i=0}$ .

The family of charge distribution evolution patterns for different  $\eta_{\tau_i=0}$  was reduced using the successive ionization model with the goal of extracting the apparent values of  $\sigma_{q \rightarrow q+1}^k$ . A distinguishing feature of the dependence  $\sigma_{q \rightarrow q+1}^k = f(\eta_{\tau_i=0})$  was that the values of  $\sigma_{q \rightarrow q+1}^k$  increase with decreasing  $\eta_{\tau_i=0}$ , asymptotically approaching some values at  $\eta_{\tau_i=0} \approx 0$ . When  $\sigma_{q \rightarrow q+1}^k$  was already practically no longer dependent of  $\eta_{\tau_i=0}$  (for  $\eta_{\tau_i=0} = 10^{-2}$ ), the ion loss rate from the trap was measured during the ionization process. In order to do this, the total ion charge in the trap  $Q^+$  and the average ion charge  $\bar{q}$  were measured as functions of the ionization time  $\tau_i$  in the absence of a background (see Fig. 3). It is seen that the ratio  $Q^+/\bar{q}$ , which constitutes the number of ions in the trap, is conserved during the entire ionization process; i.e., there is no loss of ions.

Thus, we found the conditions under which the charge distribution evolution is produced by definite batches of ions, and all the ions from the instant  $\tau_i = 0$  up to the end of the ionization process are located in the ion trap and interact with the beam of fast electrons. It is natural to regard the values of  $\sigma_{q \rightarrow q+1}$  obtained under such conditions as the true effective cross sections for ionization of positive ions by electron impact. All the

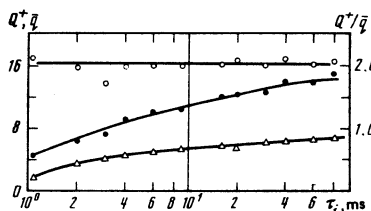


FIG. 3. The ion charge in the trap  $Q^+$  ( $\bullet$ ), the average ion charge  $\bar{q}$  ( $\Delta$ ), and the number of ions  $Q^+/\bar{q}$  ( $\circ$ ) as functions of  $\tau_i$  for  $\eta_{\tau_i=0} = 10^{-2}$ .

presented measured values of  $\sigma_{q \rightarrow q+1}$  for all the ions, except Kr and Xe, were obtained under such conditions.

## 2. EXPERIMENTAL RESULTS

1. *Carbon, nitrogen, oxygen, neon.* In order to investigate the ionization, as a rule we used molecular gases as a working substance; in particular, for ionization of carbon we used methane  $\text{CH}_4$ . Therefore in the analysis of the charge distribution evolution pattern we took as the initial distributions the charge distributions in which molecular ions were already completely absent.

All the charge distribution evolution patterns of the indicated elements are reduced by the successive-ionization model. The satisfactory agreement between the experimental charge-distribution evolutions and those regenerated from the corresponding set of  $\sigma_{q \rightarrow q+1}$  values suggests that this model in general correctly describes the process of going from lower to higher charged states (see Fig. 1). On Fig. 4 we present for C, N, O, and Ne respectively the experimental dependences of the  $\sigma_{q \rightarrow q+1}$  on the energy of the bombarding electrons.

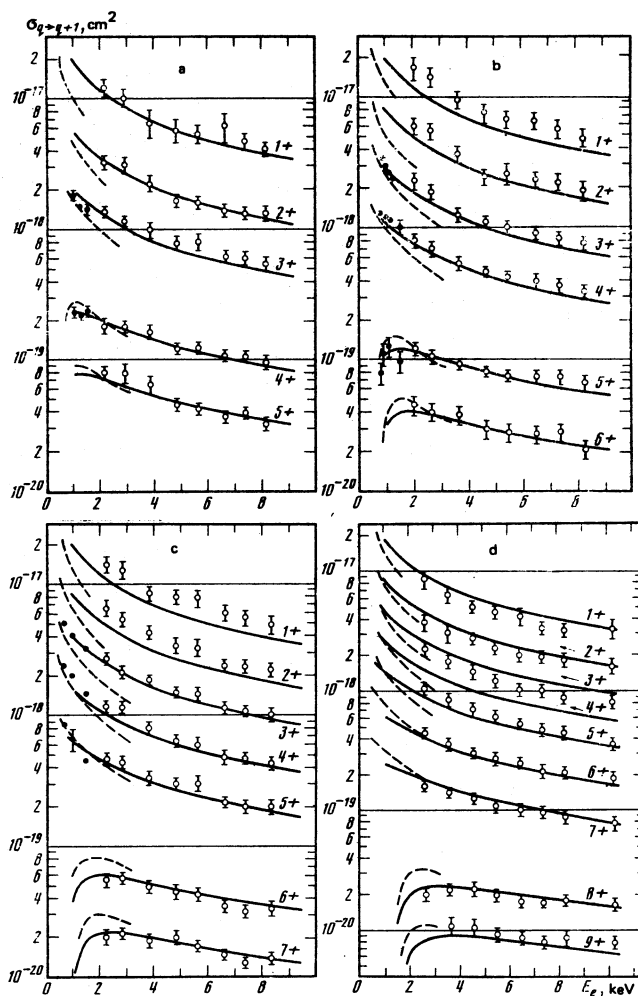


FIG. 4. Energy dependences of the  $\sigma_{q \rightarrow q+1}$  for: (a) carbon ions; (b) nitrogen ions; (c) oxygen ions; and (d) neon ions;  $\circ$ —our data,  $\bullet$ —Crandall's data<sup>8</sup>; solid lines—Salop's data<sup>22</sup>.

A detailed examination of Fig. 1 shows several systematic differences between the regenerated charge-distribution evolutions and the experimental ones. These differences are also characteristic of the charge distribution evolutions of nitrogen and other elements. The differences are that as a rule the experimental points lie somewhat higher than the corresponding  $n_q = f(j\tau_i)_{\text{regen}}$  curves in the regions of the  $j\tau_i$  values which correspond to the appearance in the spectrum of ions with charge  $q$ , and in the regions of the  $j\tau_i$  values for which the process of "burn-out" of these ions is completed. This may be considered as evidence of a two-electron ionization process, i.e., production of ions of charge  $q$  directly from ions of charge  $q-2$ . When the entire curve  $n_q = f(j\tau_i)$  is obtained in the charge distribution evolution pattern, up to practically complete "burn-out" of the ions of charge  $q$ , the process of two-electron ionization, due to the relatively small value of the cross section  $\sigma_{q-2 \rightarrow q}$ , does not substantially affect the values of  $\sigma_{q-1 \rightarrow q}$  and  $\sigma_{q \rightarrow q+1}$ ; and the successive ionization model correctly describes the entire process of going from lower to higher charge. But if the charge distribution evolution pattern is cut off at the values  $j\tau_i$  at which ions with charge  $q$  only begin to appear in the spectrum (which corresponds as a rule to  $n_{q-2}/n_{q-1} \gg 1$ ), then the two-electron ionization process may distort to one degree or another the result values of  $\sigma_{q-1 \rightarrow q}$  obtained in the successive ionization model. On the other hand, the initial parts of the  $n_q = f(j\tau_i)$  curves may be used to obtain the parameters  $\sigma_{q-r \rightarrow q}$ . In particular, for the Ne ions, in an investigation of the final section of the charge distribution evolution pattern obtained for  $E_e = 8.3$  keV, we measured the dependence

$$\frac{dn_{10}}{d(j\tau_i)} = f(j\tau_i),$$

which we compared with the curve  $n_q = f(j\tau_i)$ . We obtained some deviations from similarity of these curves, which may be explained by the direct contribution of  $\text{Ne}^{8+}$  to the formation of the  $\text{Ne}^{10+}$  ions. The analysis showed that with  $\sigma_{8 \rightarrow 10} \approx 3 \cdot 10^{-2} \sigma_{8 \rightarrow 9}$  and a 10% decrease in the value of  $\sigma_{9 \rightarrow 10}$ , this section of the experimental charge distribution evolution pattern may become more consistent with the regenerated charge distribution evolution pattern. However, for a definite determination of the values of the effective cross section of two-electron ionization, it is necessary here to increase the accuracy of the measurement of the initial sections of the curves  $n_q = f(j\tau_i)$ .

On Figs. 4a-c we also presented the results of the recent experiments of Crandall *et al.*<sup>8</sup> in the range of electron energies close to our data. It is seen that when extrapolated to the relatively small interval of  $E_e$  (~700 eV), our data and Crandall's data agree with one another despite the fact that the latter are obtained by the intersecting-beam method. This agreement may be considered as independent verification of the fact that the technique we have developed for measurement of the effective cross sections for ionization of positive ions by electron impact give quantitatively correct results.

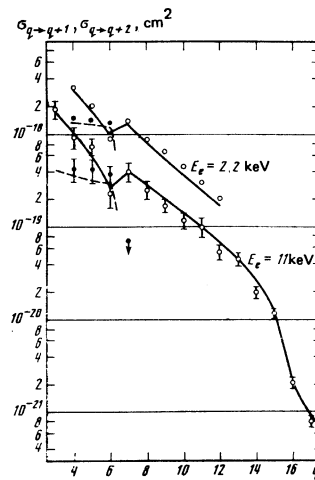


FIG. 5. Experimental values of  $\sigma_{q \rightarrow q+1}$  (○),  $\sigma_{q \rightarrow q+2}$  (●) for Ar ions of different charge  $q$ ; solid lines ( $\sigma_{q \rightarrow q+1}$ )—Lotz's data<sup>21</sup> and Salop's data<sup>23</sup>; dashed lines ( $\sigma_{q \rightarrow q+2}$ )—data from the same authors.

2. *Argon.* The argon atom, with 18 electrons in the shell, is already a rather complex system in which the number of possible ionization routes increases. Accordingly, the charge distribution evolution patterns were obtained and processed in three different intervals and, accordingly, different  $j\tau_i$  intervals: ( $2 \leq q \leq 12$ ;  $8 \leq q \leq 15$ ;  $15 \leq q \leq 18$ ) at  $E_e = 11$  keV and partially at  $E_e = 7.8$  keV. Since the charge distribution evolution pattern at 11 keV for the first of the indicated  $q$  intervals indicated the presence of a significant contribution from two-electron ionization, which was mentioned earlier,<sup>10</sup> this pattern was reduced assuming the possibility of (in addition to the fundamental transitions) also the following transitions:  $\text{Ar}^{4+} \rightarrow \text{Ar}^{6+}$ ,  $\text{Ar}^{5+} \rightarrow \text{Ar}^{7+}$ ,  $\text{Ar}^{6+} \rightarrow \text{Ar}^{8+}$ ,  $\text{Ar}^{7+} \rightarrow \text{Ar}^{9+}$ . For the remaining  $q$  intervals, the successive-ionization model was used.

The experimental results for an electron energy 11 keV are given on Fig. 5, which shows also the results of our first work,<sup>10</sup> for which the measurement errors are not indicated. At  $E_e = 7.8$  keV, we obtained the following values for the cross sections:  $\sigma_{15 \rightarrow 16} = (1.40 \pm 0.21) \cdot 10^{-20}$  cm<sup>2</sup>,  $\sigma_{16 \rightarrow 17} = (1.75 \pm 0.25) \cdot 10^{-21}$  cm<sup>2</sup>,  $\sigma_{17 \rightarrow 18} = (7.4 \pm 0.9) \cdot 10^{-22}$  cm<sup>2</sup>.

3. *Krypton, xenon.* In the ionization of Kr and Xe, natural isotopic mixtures were used. For Kr, we obtained the charge distribution evolution pattern at  $E_e = 8.5$  keV and in the range of values  $6 \leq q \leq 34$  (Ref. 18); for Xe also at  $E_e = 8.5$  keV and in the range  $9 \leq q \leq 44$  (Ref. 18) and at  $E_e = 18$  keV and  $9 \leq q \leq 48$  (Ref. 19). Insufficiently good resolution of the lines at  $q > 10-15$  was characteristic for the charge spectra in these cases. Accordingly, we obtained from the charge distribution evolution patterns plots of the average charge of the ions  $\bar{q}$  vs. the factor  $j\tau_i$ . If we assume that the condition for the increase in the average ionic charge by unity is the relationship  $\sigma_{\bar{q} \rightarrow \bar{q}+1}(\Delta j\tau_i) = 1$  (meaning a unity probability of collision of an electron with an ion at an effective cross section  $\sigma_{\bar{q} \rightarrow \bar{q}+1}$ ), then it is easy to obtain from such plots the dependences of  $\sigma_{\bar{q} \rightarrow \bar{q}+1}$  on  $q$ . The results for Kr and Xe are presented

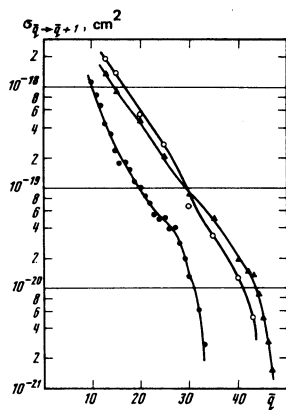


FIG. 6. Experimental values of the effective  $\sigma_{\bar{q} \rightarrow \bar{q}+1}$  for the Kr ions ( $\bullet$ ,  $E_0 = 8.5$  keV) and Xe ( $\circ$ ,  $E_0 = 8.5$  keV;  $\blacktriangle$ ,  $E_0 = 18$  keV) of different charges  $\bar{q}$ .

on Fig. 6. Of course, using such an approach, the irregularities connected with the presence of shells are lost to a significant degree. Furthermore, the values obtained for the effective ionization cross sections contain inaccuracies connected with the incomplete character of the ionization model. Nevertheless, the values of  $\sigma_{\bar{q} \rightarrow \bar{q}+1}$  for such a large number of highly charged Kr and Xe ions are obtained experimentally and may be of definite value primarily for further development of work on ionization.

### 3. ANALYSIS OF RESULTS, COMPARISON WITH THEORY

It is of interest to compare our experimental curves of the energy dependences of the ionization cross sections of hydrogen-like ions of C, N, O, Ne, and Ar with the theoretical dependences found by the Coulomb-Born method<sup>20</sup> within the framework of the relation

$$Z^4 \sigma_{z-1 \rightarrow z} = f(E_e/I),$$

where  $I$  is the ionization potential of a hydrogen-like ion from the  $1s$  state and  $Z$  is the nuclear charge.

On Fig. 7, the solid line shows the results of a calculation by the KBO method for  $Z = 128$ . It shows also all our experimental points for the cross sections for the  $Z-1 \rightarrow Z$  transitions in hydrogen-like ions of the indicated elements. It is seen that the quantitative agree-

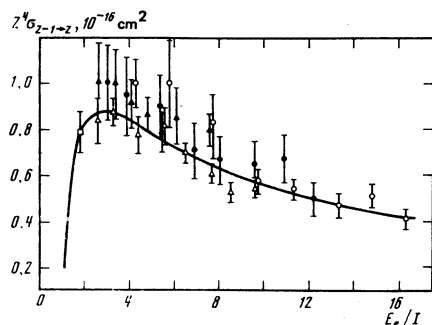


FIG. 7. The dependence of the reduced ionization cross sections of hydrogen-like ions on the electron energy;  $\circ$ — $C^{5+}$ ,  $\bullet$ — $N^{6+}$ ,  $\Delta$ — $O^{7+}$ ,  $\blacktriangle$ — $Ne^{9+}$ ,  $\square$ — $Ar^{17+}$ , solid line—calculation<sup>20</sup> for  $Z = 128$ .

ment between experiment and theory is not bad. But we observe also some deviation whose average over the entire set of experimental points tends toward values of  $Z^4 \sigma_{z-1 \rightarrow z}$  equals about the average error of the measurements.

The level of accuracy of the experimental points does not allow us at present to extract the dependence of the given cross section on nuclear charge. However, the problem of the experimental investigation of this dependence may be posed and solved. For this it is necessary first of all to increase the accuracy of the measurement of the initial sections of the  $n_q = f(j\tau_i)$  curves, so that the two-electron ionization of helium-like ions can be taken into account and the accuracy of the  $\sigma_{1s \rightarrow k}$  measurement may thus be increased.

For helium-like and other up to boron-like ions, we also observe good agreement of the experimental points with the values of  $\sigma_{q \rightarrow q+1}$  calculated from the Lotz formula,<sup>21</sup> and an appreciable deviation from the Salop calculation.<sup>22</sup> This means that for the indicated ions in the energy range under consideration, the successive one-electron ionization model describes with sufficient accuracy the transition from lower to higher charged states. But for ions with more than 5 shell electrons, we observe a systematic excess of the experimental results over the calculated values; this deviation can be reduced by taking into account the contribution of two-electron ionization. As regards Kr and Xe, the values of  $\sigma_{\bar{q} \rightarrow \bar{q}+1}$  obtained experimentally represent some effective values which correctly describe the dynamics of the motion of the most probable values of  $\bar{q}$  along the  $j\tau_i$  axis during the ionization process. These values may be used for various kinds of estimates of the ionization factor necessary to obtain ions with the corresponding charges.

In the reduction of the charge distribution evolution pattern of Ar ions close to  $q = 8$ , we used the two-electron ionization model; this made it also possible to obtain the values of  $\sigma_{4 \rightarrow 6}$ ,  $\sigma_{5 \rightarrow 7}$ ,  $\sigma_{6 \rightarrow 8}$ . This proved to be possible at present levels of accuracy of the measurements, thanks to the relatively large contribution made to the ionization cross sections of  $Ar^{4+}$ ,  $Ar^{5+}$ , and  $Ar^{6+}$  by the probability of the onset of vacancies in the  $L$  shell. But for a systematic study of many-electron ionization, it is necessary to increase the accuracy with which the experimental charge distribution evolution patterns are obtained and to make the measurement process automatic. However, even now we may note that close to large shells, a situation is realized in which  $\sigma_{q \rightarrow q+1}$  may prove to be smaller than  $\sigma_{q+1 \rightarrow q+2}$ , and even smaller than  $\sigma_{q \rightarrow q+2}$ . An explanation for this phenomenon can be given if the Salop model<sup>23</sup> is valid; this indicates that the removal of an electron from the  $L$  shell to the continuum leads with high probability to the ejection of still another electron, if there are two or more of them in the  $M$  shell. On Fig. 5 we give the values of  $\sigma_{q \rightarrow q+1}$  (solid curve) and  $\sigma_{q \rightarrow q+2}$  (dashed curve) calculated from the Lotz formula and corrected assuming validity of the Salop model. We should point out the rather good agreement between experiment and calculation. In the calculation, the auto-

ionization process upon excitation of the  $L$  electrons is not taken into account.

In conclusion, the authors owe their thanks to V. G. Dudnikov, V. V. Sal'nikov, and A. P. Suslov for participation in the preparation for and performance of the measurements, and also to S. V. Kartashov for participation in the reduction of the experimental data.

- <sup>1</sup>V. A. Bazylev and M. I. Chibisov, Preprint IAÉ-3125, Moscow (1979).  
<sup>2</sup>V. A. Bazylev and M. I. Chibisov, Preprint IAÉ-3152, Moscow (1979).  
<sup>3</sup>J. B. Hasted, *Physics of Atom Collisions*, Butterworths, Washington, 1964. (Russ. Transl., Mir, Moscow, 1965).  
<sup>4</sup>G. H. Dunn, *IEEE Trans. Nucl. Sci.* NS23, 929 (1976).  
<sup>5</sup>K. L. Aitken and M. F. A. Harrison, *J. Phys.* B4, 1176 (1971).  
<sup>6</sup>S. O. Martin, B. Peart, and K. T. Dolder, *J. Phys.* B1, 537 (1968).  
<sup>7</sup>P. Mahadevan, VI ICPEAC, Cambridge, Massachusetts, 1969, p. 337.  
<sup>8</sup>D. H. Crandall, R. A. Phaneuf, and D. C. Gregory, ORNL/

- TM-7020, 1979.  
<sup>9</sup>E. D. Donets and V. P. Ovsyannikov, *JINR*, R7-9799, Dubna, 1976.  
<sup>10</sup>E. D. Donets and A. I. Pikin, *Zh. Eksp. Teor. Fiz.* 70, 2025 (1976) [*Sov. Phys. JETP* 43, 1057 (1976)].  
<sup>11</sup>E. D. Donets and A. I. Pikin, *Zh. Tekh. Fiz.* 45, 2373 (1975) [*Sov. Phys. Tech. Phys.* 20, 1477 (1975)].  
<sup>12</sup>E. D. Donets and V. P. Ovsyannikov, *JINR*, R-10780, Dubna, 1977.  
<sup>13</sup>B. Bochev, T. Kutsarova, and V. P. Ovsyannikov, *JINR*, R5-11566, Dubna, 1978.  
<sup>14</sup>B. Bochev, V. P. Ovsyannikov, and T. Kutsarova, *JINR*, R7-11567, Dubna, 1978.  
<sup>15</sup>L. Aleksandrov, *JINR*, R5-10366, Dubna, 1977.  
<sup>16</sup>L. Aleksandrov, *JINR*, R5-7259, Dubna, 1973.  
<sup>17</sup>L. Aleksandrov, *JINR*, B1-59969, Dubna, 1976.  
<sup>18</sup>N. N. Blinnikov *et al.*, *JINR*, 9-12409, Dubna, 1977.  
<sup>19</sup>E. D. Donets, V. P. Ovsyannikov, and V. G. Dudnikov, *JINR*, R7-12905, Dubna, 1979.  
<sup>20</sup>M. R. H. Rudge and S. B. Schwartz, *Proc. Phys. Soc.* 88, 563 (1966).  
<sup>21</sup>W. Lotz, *J. Opt. Soc. Am.* 57, 873 (1967).  
<sup>22</sup>A. Salop, *Phys. Rev.* A14, 2095 (1976).  
<sup>23</sup>A. Salop, *Phys. Rev.* A9, 2496 (1974).

Translated by Cathy Flick

## Quantum theory of Stark broadening of the lines of hydrogenlike ions

F. F. Baryshenkov and V. S. Lisitsa

*I. V. Kurchatov Atomic Energy Institute*

(Submitted 19 May 1980)

*Zh. Eksp. Teor. Fiz.* 80, 926-932 (March 1981)

An exact analytic solution of the problem of hydrogenlike-ion line broadening by electrons is obtained within the framework of the dipole approximation. The character of the solution is investigated at various values of the Coulomb parameter  $Ze^2/\hbar v$ . The transition to solutions for a neutral atom is tracked, as well as that to the impact theory of broadening, including its classical limit.

PACS numbers: 32.60.+i, 32.70.Jz

### §1. INTRODUCTION

The recent development of the theory of the hydrogen-atom (H) and of  $H$ -like-ion line broadening<sup>1-4</sup> was based on the use of the specific properties of the Coulomb symmetry of  $H$ -like systems, wherein the line contour could be described not only at high and low frequencies  $\Delta\omega$ , but also in the intermediate  $\Delta\omega$  region. For neutral hydrogen, the line contours were calculated both in the classical<sup>1</sup> and in the quantum<sup>3,4</sup> cases. The situation here is analogous in many respects to nonrelativistic theory of bremsstrahlung in a Coulomb field, where classical and quantum solutions and the relations between them are also known.<sup>5</sup> Calculations of the line contours of  $H$ -like ions are known in the impact limit,<sup>6</sup> as well as in the intermediate frequency region,<sup>2</sup> but only in the classical-trajectory approximation.

We obtain in this paper general quantum solutions for the line contours of  $H$ -like ions, and investigate their

connection with the known limiting cases. A new parameter of the problem compared with the case of neutral hydrogen is the parameter  $Ze^2/\hbar v$ , where  $Z$  is the ion charge and  $v$  is the velocity of the particle that causes the broadening. We note that allowance for the quantum effects is more important for  $H$ -like ions than for neutral hydrogen (see Ref. 7, Chap. 4). The reason is the decrease of the effective collision radius (the so-called Weisskopf radius<sup>8</sup>) with increasing  $Z$ . It is interesting that the theory developed is similar in many respects to the relativistic bremsstrahlung theory.<sup>9</sup>

### §2. WAVE FUNCTION OF BROADENING PARTICLE AND FORMAL EXPRESSION FOR THE LINE CONTOUR

The line contour of a radiating atom or ion can be expressed in terms of the overlap integrals of the broadening particles, assumed for the sake of argument to be electrons.<sup>4</sup> Of interest for the broadening particles are